Combining Photoluminescence and Photocurrent Measurements to Distinguish Photovoltaic Losses

T. H. Gfroerer[1], Ben Stroup[1], Collin J. C. Epstein[1], Yong Zhang[2], and Zhiqiang Liu[3]

[1] Davidson College, Davidson, NC 28035, USA
[2] University of North Carolina at Charlotte, Charlotte, NC 28223, USA
[3]Institute of Semiconductors, Chinese Academy of Science, Beijing, 100086, CHINA

***Abstract* — We measure the photoluminescence and photocurrent of a blue LED under open- and short-circuit conditions to distinguish between drift and non-drift related carrier loss mechanisms. We also vary the excitation intensity and temperature to monitor changes in recombination parameters. Using a simple rate equation model, we find that diffusion-related non-radiative recombination is thermally activated with an activation energy equal to approximately 44 meV, while drift-related losses account for an excitation- and temperature-independent 10% short-circuit current deficit when the carrier density exceeds a threshold of 5×10^{14} cm^{-3}.**

I. Introduction

Non-radiative recombination limits the performance of all semiconductor devices. Recombination centers can occur in a variety of forms, from microscopic point defects to extended features like dislocations and mismatched heterojunctions. But charge carriers must travel to reach these centers. Hence, we may be able to control recombination losses if we know how the charge carriers move to the recombination sites.

Charge carrier transport can be separated into two general categories: diffusion and drift. Diffusion is driven by random motion and concentration gradients – carriers tend to move from high concentration regions to low concentration regions so the multiplicity of configurations increases in accordance with the second law of thermodynamics. In contrast, drift is driven by electric fields, like the built-in field across the p-n junction of a diode. Most carriers in an operational semiconductor device exhibit a combination of both modes of transport.

In this investigation, we seek to distinguish between diffusion- and drift-related contributions to photovoltaic losses. We accomplish this task by comparing the steady-state response under open- and short-circuit conditions. For a stand-alone device with no external circuit, there is no net drift of free carriers through the device in steady-state. But when the device is short-circuited, carriers will drift through the device and contribute to current around the circuit. We compare the photoluminescence intensity that is emitted by the device under open- and short-circuit conditions, carefully accounting for carriers that contribute to the current in the short-circuit case. Our analysis quantifies the augmented losses associated with the short-circuit drift.

II. Experiment

Our test device for demonstrating this characterization technique is a high-brightness blue LED. A similar study has been reported on this type of device, [1] but the authors did not use temperature to examine thermal effects. The structure consists of n-GaN, several InGaN/GaN quantum wells (QWs), and p-GaN grown on a sapphire substrate. Details are comparable to those of Device B described in Reference [2]. The device is mounted in an Oxford Instruments Optistat DN cryostat and illuminated by an AixiZ 405nm, 150 mW laser. The beam quality of this extremely economical diode laser is far from ideal: the low-quality output coupler produces a ring-shaped pattern, which we focus to a diameter of approximately 0.6mm centered on the 1mm × 1mm device. Representative images of the photoluminescence pattern are shown in Fig. 1.

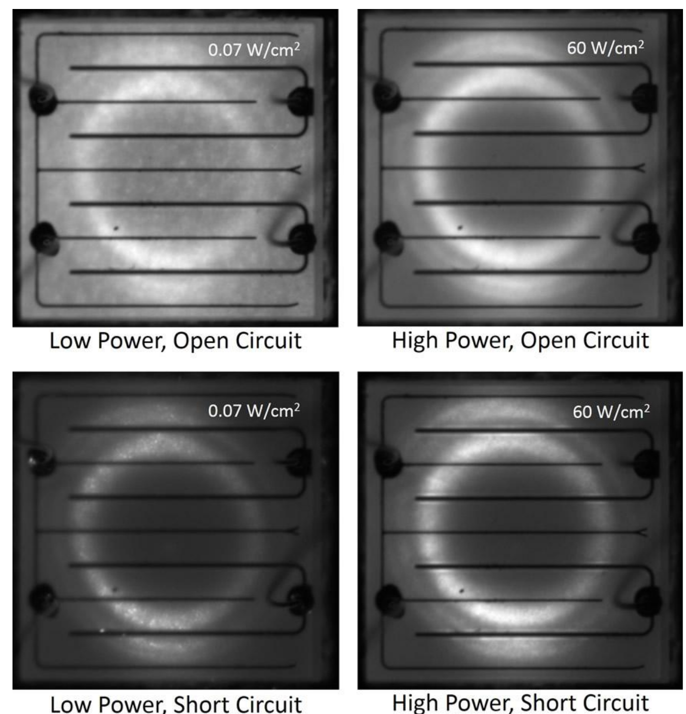

Fig. 1. Representative photoluminescence images showing the inhomogeneous excitation pattern (Temperature = 155K). The excitation estimates noted on each image are obtained by dividing the incident laser power by the illuminated region of the device.

The laser intensity is controlled with a set of New Focus 5215 neutral density filter wheels. A pair of lenses direct the integrated photoluminescence to a New Focus 2031 Large Area Photoreceiver with a GG435 long-pass colored glass filter to eliminate scattered laser light. For short-circuit experiments, a Keithley 2400 SourceMeter set to source zero volts is used to measure the short-circuit current.

III. RESULTS

The free-carrier generation rate G depends on the incident laser power (corrected for reflections), the fraction absorbed, the photon energy, and the excitation area. Absorption calculations are difficult because, in addition to the active QWs, the device structure includes several other layers with potentially significant absorption. In particular, we estimate that sub-bandgap absorption in the 2 μm n-GaN buffer could capture up to 30% of the incident light. [3] Meanwhile, absorption measurements are complicated by scattering from the patterned growth plane and at the unpolished bottom surface of the substrate. Since a minimum of 50% absorption is required to account for the short-circuit current output at maximum photovoltaic quantum efficiency, we employ this lower bound in our analysis. To estimate the excitation area, we use a high-contrast photoluminescence image (like the high-power, short circuit image in Fig. 1), where pixels with counts exceeding half of the maximum are considered illuminated. Fig. 2 shows how the normalized photovoltaic quantum efficiency (i.e. the current out divided by the free-carrier generation rate) depends on excitation.

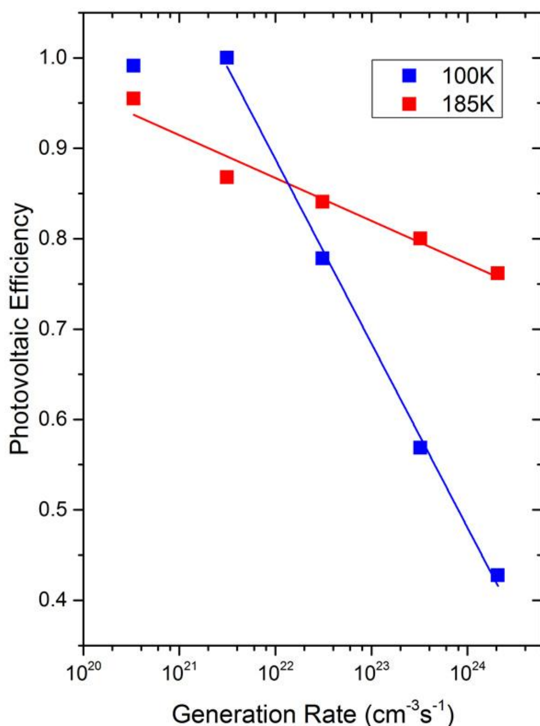

Fig. 2. Normalized photovoltaic quantum efficiency vs. the rate of electron-hole pair generation under short-circuit conditions at two temperatures (100K and 185K). The solid lines are only linear guides to the eye.

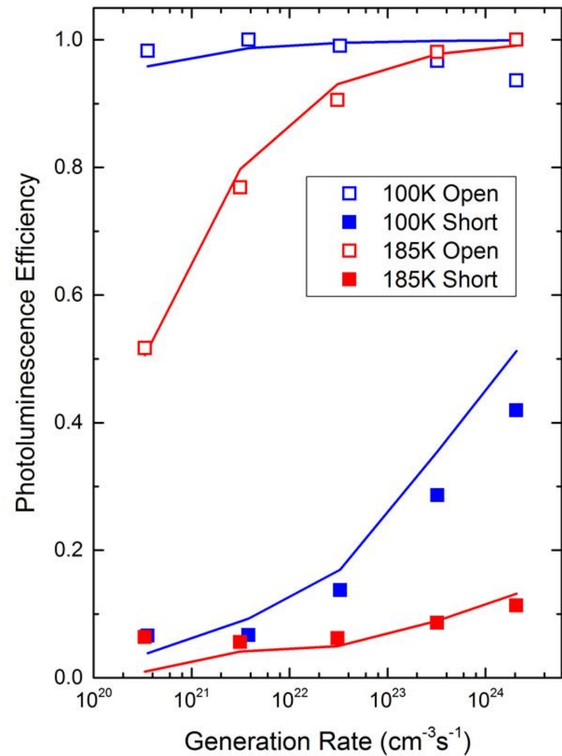

Fig. 3. Radiative efficiency vs. the rate of electron-hole pair generation under open- and short-circuit conditions at 100K and 185K. The solid lines are theoretical calculations based on the model described in the Section IV.

A relative measure of the radiative efficiency is given by the ratio of the integrated photoluminescence signal and the incident laser intensity. But under open-circuit conditions at 100K, we note that the radiative efficiency is relatively constant as the photoexcitation intensity is varied by nearly four orders of magnitude. We also note that the open-circuit efficiency at 185K approaches a comparable level at high excitation. Hence, we assume that this level corresponds to approximately 100% internal radiative efficiency and we normalize our other measurements accordingly. The calibrated radiative efficiency data is shown in Fig. 3.

IV. ANALYSIS

The reduction of photovoltaic efficiency with increasing generation rate correlates well with the accompanying increase in radiative efficiency, indicating that our scaling procedure is relatively accurate. The solid lines in Fig. 3 are the results of a more quantitative rate equation analysis of the experimental results. Since all measurements are conducted in steady-state, we employ the following relations:

$$\frac{dn}{dt} = G - Bn^2 - A_d(T)n = 0 \quad (1)$$

$$\frac{dn}{dt} = G - Bn^2 - \frac{I_{SC}}{qV} - \left(\frac{n - N_I}{n}\right)\frac{I_{SH}}{qV} = 0 \quad (2)$$

where (1) is used for open-circuit and (2) is used for short-circuit conditions. In these expressions, n is the density of free carriers, B is the radiative recombination coefficient, $A_d(T)$ is a temperature-dependent diffusive non-radiative recombination coefficient, I_{SC} is the measured short-circuit current out, qV is the product of the electron charge and active device volume, I_{SH} is shunt current loss, [4] and N_I is a density threshold for the shunt current mechanism (when $n < N_I$, I_{SH} is set to zero).

We start with a room-temperature radiative recombination coefficient of $B = 3 \times 10^{-11}$ cm^3/s, [5] which may include photon recycling, and correct for temperature by assuming that B is proportional to $T^{-3/2}$. [6] Above a small carrier density threshold ($N_I = 5 \times 10^{14}$ cm^{-3}), the photovoltaic efficiency experiences an abrupt drop and a density-activated shunt current mechanism is required to fit the short-circuit measurements. Presumably, carriers are localized in less defective channels, reducing leakage when $n < N_I$. [2] This excitation- and temperature-independent drift-related loss mechanism eliminates 10% of the short circuit current (i.e. $I_{SH} = 0.1 I_{SC}$) for carrier densities exceeding N_I.

At each temperature, open-circuit experimental results for photoexcitation conditions varying by nearly four orders of magnitude are modeled according to Eq. 1, with A_d as the only adjustable parameter. As shown in Fig. 4, this diffusive (i.e. non-drift related) non-radiative recombination coefficient depends strongly on temperature, with a thermal activation energy of 44 meV. This quantity is roughly half the LO phonon energy (87 meV) deduced from phonon replicas in the emission spectrum. Curiously, we obtain lower error when the SRH-type recombination mechanism [7] is omitted from the short-circuit model, suggesting that this non-radiative process does not play a significant role when the carriers drift. Motion along the direction of the internal field may preclude capture at the diffusion-related recombination centers that dominate in the open-circuit configuration. The deviation between experiment and theory at 100K in the high generation regime can be attributed to efficiency droop, which sets in at lower excitation when the device is cold. [2,5] The specific loss mechanism associated with efficiency droop in these kinds of devices remains subject to debate.

Our analysis indicates that the decrease in radiative efficiency with increasing temperature for the low excitation, open-circuit configuration is due to an increase in diffusive non-radiative recombination. Meanwhile, the decrease in radiative efficiency with increasing temperature for the high-excitation, short-circuit configuration can be attributed to the decrease in the radiative recombination rate. And above a relatively low excitation threshold, a systematic 10% loss of drifting carriers accompanies the current flow in the short-circuit configuration. We find that combining photoluminescence with photocurrent measurements over a wide range of temperatures and excitation conditions enables us to identify and characterize three contributions to carrier dynamics in the device, namely: radiative recombination, diffusive non-radiative recombination, and drift-related current loss. The complementary techniques yield a more thorough characterization protocol, which may facilitate technology that improves future device performance.

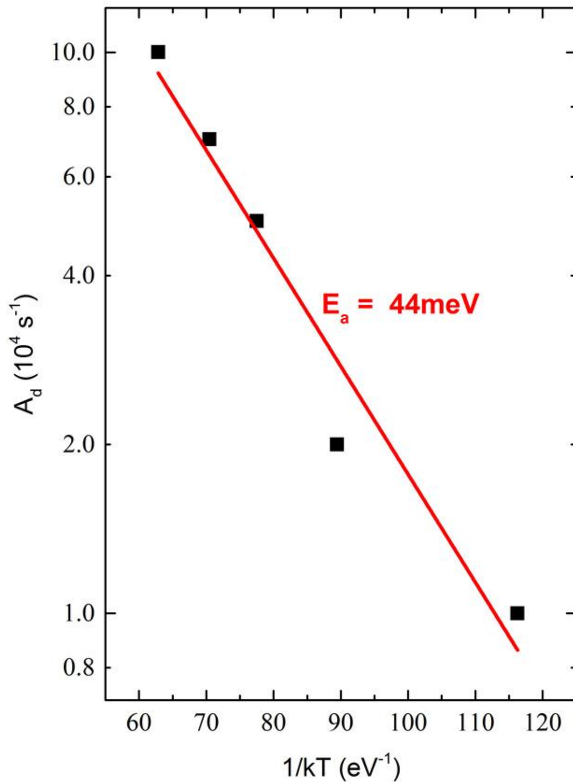

Fig. 4. Arrhenius plot of the temperature-dependent non-radiative recombination coefficient A_d that is used to fit the open-circuit results. The slope yields a thermal activation energy of approximately 44 meV.

REFERENCES

[1] Seung-Hyuk Lim, Young-Ho Ko and Yong-Hoon Cho, "A quantitative method for determination of carrier escape efficiency in GaN-based light-emitting diodes: A comparison of open- and short-circuit photoluminescence," *Appl. Phys. Lett.* **104**, 091104 (2014).

[2] Yue Lin, Yong Zhang, Zhiqiang Liu, Liqin Su, Jihong Zhang, Tongbo Wei, and Zhong Chen, "Interplay of point defects, extended defects, and carrier localization in the efficiency droop of InGaN quantum wells light-emitting diodes investigated using spatially resolved electroluminescence and photoluminescence," *J. Appl. Phys.* **115**, 023103 (2014).

[3] O. Ambacher, W. Rieger, P. Ansmann, H. Angerer, T.D. Moustakas, and M. Stutzmann, "Sub-bandgap absorption of Gallium Nitride determined by photothermal deflection spectroscopy," *Solid State Commun.* **97**, 365 (1996).

[4] Jenny Nelson, *The Physics of Solar Cells.* London: Imperial College Press, 2003.

[5] J. Hader, J. V. Moloney, and S. W. Koch, "Temperature-dependence of the internal efficiency droop in GaN-based diodes," *Appl. Phys. Lett.* **99**, 181127 (2011).

[6] T.H. Gfroerer, L.P. Priestley, M.F. Fairley, and M.W. Wanlass, "Temperature dependence of nonradiative recombination in low-bandgap InGaAs/InAsP double-heterostructures grown on InP substrates," *J. Appl. Phys.* **94**, 1738 (2003).

[7] W. Shockley and W. T. Read, Jr., *Phys. Rev.* **87**, 835 (1952); R. N. Hall, *ibid.* **87**, 387 (1952).